Modified Phthalocyanines for Efficient Near-IR Sensitization of Nanostructured TiO$_2$ Electrode

Jianjun He,[†] Gábor Benkö,[†] Ferenc Korodi,[‡] Tomás Polívka,[†] Reiner Lomoth,[§]
Björn Åkermark,[‡] Licheng Sun,*,[‡] Anders Hagfeldt,[§] and Villy Sundström*,[†]

*Contribution from the Department of Chemical Physics, Lund University, S-221 00 Lund,
Sweden, Department of Organic Chemistry, Stockholm University, S-106 91 Stockholm, Sweden,
and Department of Physical Chemistry, Uppsala University, S-751 21 Uppsala, Sweden*

Received December 18, 2001

Abstract: A zinc phthalocyanine with tyrosine substituents (ZnPcTyr), modified for efficient far-red/near-IR performance in dye-sensitized nanostructured TiO$_2$ solar cells, and its reference, glycine-substituted zinc phthalocyanine (ZnPcGly), were synthesized and characterized. The compounds were studied spectroscopically, electrochemically, and photoelectrochemically. Incorporating tyrosine groups into phthalocyanine makes the dye ethanol-soluble and reduces surface aggregation as a result of steric effects. The performance of a solar cell based on ZnPcTyr is much better than that based on ZnPcGly. Addition of 3α,7α-dihydroxy-5β-cholic acid (cheno) and 4-*tert*-butylpyridine (TBP) to the dye solution when preparing a dye-sensitized TiO$_2$ electrode diminishes significantly the surface aggregation and, therefore, improves the performance of solar cells based on these phthalocyanines. The highest monochromatic incident photo-to-current conversion efficiency (IPCE) of ~24% at 690 nm and an overall conversion efficiency (η) of 0.54% were achieved for a cell based on a ZnPcTyr-sensitized TiO$_2$ electrode. Addition of TBP in the electrolyte decreases the IPCE and η considerably, although it increases the open-circuit photovoltage. Time-resolved transient absorption measurements of interfacial electron-transfer kinetics in a ZnPcTyr-sensitized nanostructured TiO$_2$ thin film show that electron injection from the excited state of the dye into the conduction band of TiO$_2$ is completed in ~500 fs and that more than half of the injected electrons recombines with the oxidized dye molecules in ~300 ps. In addition to surface aggregation, the very fast electron recombination is most likely responsible for the low performance of the solar cell based on ZnPcTyr.

Introduction

The dye-sensitized photoelectrochemical solar cell (DSSC) is one of the recent possibilities of harvesting solar energy by converting it into electricity. The heart of this cell is a photoanode, which is based on a nanoporous nanocrystalline, commonly called nanostructured, TiO$_2$ film covered by a monolayer of a sensitizing dye.[1-3] Upon light excitation, the adsorbed dye molecules inject electrons from their excited states into the conduction band of the semiconductor. The electrons are brought back to the oxidized dye through an external circuit, a platinum counter electrode, and a redox system (typically I$^-$/I$_3^-$). The use of a nanostructured TiO$_2$ film together with the Ru(dcbpy)$_2$(NCS)$_2$ [dcbpy = 4,4′-dicarboxy-2,2′-bipyridine] (RuN3 for short) dye introduced by Grätzel and co-workers[1,2] was a breakthrough in terms of a commercial application. An overall conversion efficiency of ~10% has been achieved. Since then, extensive attention has been paid to this research field.[4]

The DSSC is a sophisticated system, which is not yet understood in detail. To increase the conversion efficiency as well as the stability, almost all the elements of the solar cell device need further improvement. As for the sensitizing dye, there are several theoretical requirements that it has to comply with.[5] First, the lowest unoccupied molecular orbital (LUMO) of the dye should have a higher energy than the conduction band edge of the semiconductor and have a good orbital overlap to facilitate electron injection. Ideally, the dye should have intensive absorption in the whole solar spectrum. Second, the dye should be attached strongly to the semiconductor surface and inject electrons into the conduction band with a quantum yield of unity, while the charge recombination between the injected electron and the oxidized dye should be slow enough for the electron transport to the external circuit. Third, the redox

* Corresponding author. E-mail: Villy.Sundstrom@chemphys.lu.se.
† Lund University.
‡ Stockholm University.
§ Uppsala University.

(1) O'Regan, B.; Grätzel, M. *Nature* **1991**, *353*, 737.
(2) Nazeeruddin, M. K.; Kay, A.; Rodicio, I.; Humphry-Baker, R.; Müller, E.; Liska, P.; Vlachopoulos, N.; Grätzel, M. *J. Am. Chem. Soc.* **1993**, *115*, 6382.
(3) Hagfeldt, A.; Grätzel, M. *Chem. Rev.* **1995**, *95*, 49.
(4) For example: (a) Hagfeldt, A.; Grätzel, M. *Acc. Chem. Res.* **2000**, *33*, 269. (b) Kelly, C. A.; Meyer, G. J. *Coord. Chem. Rev.* **2001**, *211*, 295. (c) Bonhôte, P.; Moser, J.-E.; Humphry-Baker, R.; Vlachopoulos, N.; Zakeeruddin, S. M.; Walder, L.; Grätzel, M. *J. Am. Chem. Soc.* **1999**, *121*, 1324. (d) Kalyanasundaram, K.; Grätzel, M. *Coord. Chem. Rev.* **1998**, *77*, 347. (e) Huang, S. Y.; Schlichthörl, G.; Nozik, A. J.; Grätzel, M.; Frank, A. J. *J. Phys. Chem. B* **1997**, *101*, 2576. (f) Hara, K.; Sayama, K.; Ohga, Y.; Shinpo, A.; Suga, S.; Arakawa, H. *Chem. Commun.* **2001**, 569. (g) Schwarzburg, K.; Willig, F. *J. Phys. Chem. B* **1999**, *103*, 5743.
(5) Nazeeruddin, M. K.; Péchy, P.; Renouard, T.; Zakeruddin, S. M.; Humphry-Baker, R.; Comte, P.; Liska, P.; Cevey, L.; Costa, E.; Shklover, V.; Spiccia, L.; Deacon, G. B.; Bignozzi, C. A.; Grätzel, M. *J. Am. Chem. Soc.* **2001**, *123*, 1613.

potential of the dye should be sufficiently more positive than that of the redox couple in the electrolyte so that the dye can be regenerated rapidly by electron transfer from the reduced species in the electrolyte. Finally, the dye should be chemically stable for long time exposure to natural sunlight. Another, mainly practical, requirement is that the dye should be soluble in solvents that are compatible with the semiconductor and favorable for adsorption of a nonaggregated monolayer of the dye on the nanoparticle surface. This latter requirement is important because the dye molecules that are connected directly to the semiconductor are more effective in injecting electrons into the semiconductor as compared to those in outer layers. For an aggregated sensitizer, the excess of dye molecules absorbs light and acts as a filter. Since it is very difficult to calculate all the necessary parameters and then synthesize a dye fulfilling all of them, the method of "trials and failures" is still an important approach to finding appropriate sensitizing dyes.

To date, ruthenium(II) polypyridyl complexes have proved to be the best sensitizers for dye-sensitized nanostructured TiO_2 solar cells.[1,2] However, the main drawback of those sensitizers is the lack of absorption in the far-red/near-IR region of the solar spectrum.[5] To further improve the performance of these devices, it is imperative to enhance their response in the above-mentioned wavelength region. Phthalocyanines possess intensive absorption in the far-red/near-IR region; are known for their excellent chemical, light, and thermal stability; and have the appropriate redox properties for sensitization of large band-gap semiconductors, e.g., TiO_2,[6] making them attractive for DSSC. However, there are some problems to be solved for phthalocyanines to be used in solar cell applications. The typical phthalocyanines explored for sensitization of large band-gap semiconductors are free-base or metallic ones, substituted by carboxylic or sulfonic acid groups for attachment to the semiconductor surface.[7] They are poorly soluble in organic solvents, for example, ethanol and chloroform, which makes it difficult to synthesize, separate, and purify these kinds of phthalocyanines. Another major problem with phthalocyanines is their strong tendency to aggregate on the semiconductor surface, which to some extent results in very low IPCE (typically <4%) of solar cells.[7] Grätzel and co-workers[8] reported a strikingly high IPCE of 45% in the near-infrared region for a sandwich solar cell based on a zinc tetracarboxyl phthalocyanine (ZnTcPc)-sensitized nanostructured TiO_2 electrode when surface aggregation of the sensitizer was avoided. In contrast to the typical phthalocyanines with carboxyl groups, phthalocyanines with ester groups[9] are readily synthesized and purified in good yields, as they are reasonably soluble in moderately polar solvents, for example, chloroform. However, they could not be attached to nanostructured TiO_2 film by means of ordinary methods.[2] Moreover, they were surprisingly resistant toward

Chart 1
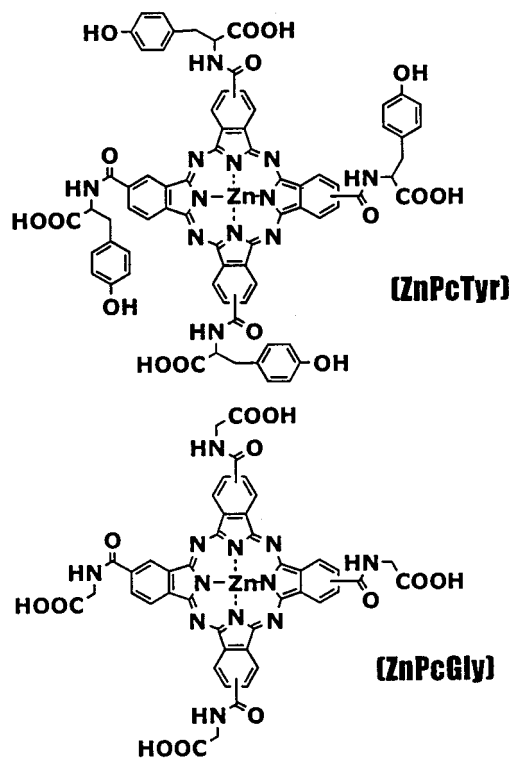
hydrolysis by, for example, NaOH. Recently, we[9] reported a novel method to attach phthalocyanines substituted by ester groups to nanostructured TiO_2 film by pretreatment of the TiO_2 film with a Lewis base ($(CH_3)_3COLi$). The highest IPCE for a TiO_2 electrode coated by a zinc phthalocyanine substituted by four ester groups (ZnPcBu) was 4.3% at 690 nm.[9] In our present study, a zinc phthalocyanine substituted with tyrosine groups (ZnPcTyr; see molecular structure in Chart 1) was modified for efficient far-red/near-IR sensitization of a nanostructured TiO_2 solar cell electrode. This compound and a reference, zinc phthalocyanine with glycine substituents (ZnPcGly; see molecular structure in Chart 1), were synthesized and characterized. The substituted phthalocyanines are more easily synthesized, separated, and purified in good yields than typical phthalocyanines,[7,8] since they can be obtained readily by hydrolysis from their corresponding esters, which are separated to high purity by means of column chromatography. Because of the incorporation of tyrosine groups into the macrocycle of zinc phthalocyanine, ZnPcTyr has a good solubility in ethanol, which is a typical solvent for sensitizers when preparing dye-sensitized nanostructured TiO_2 electrodes. Substituting tyrosine groups into phthalocyanine reduces considerably surface aggregation as a result of steric effects. It has been found recently[10] that tyrosine plays an important role in the photosynthetic oxygen-evolving photosystem II (PSII) reaction center; i.e., after a multistep downhill photoinduced electron transfer, the oxidized chlorophyll special pair (P_{680}^+) recaptures an electron by oxidizing a nearby tyrosine to a tyrosyl radical, which then abstracts a hydrogen atom from a water molecule coordinated to a manganese cluster. Therefore, another potential function of incorporating redox-active tyrosine

(6) *Phthalocyanines: Properties and applications;* Leznoff, C. C., Lever, A. B. P., Eds.; VCH: New York, 1993 (Vol. 1), 1993 (Vol. 2), 1993 (Vol. 3), 1996 (Vol. 4).

(7) (a) Fang, J.; Su, L.; Wu, J.; Shen, Y.; Lu, Z. *New J. Chem.* **1997**, *21*, 1303. (b) Shen, Y.; Wang, L.; Lu, Z.; Wei, Y.; Zhou, Q.; Mao, H.; Xu, H. *Thin Solid Films* **1995**, *257*, 144. (c) Fang, J.; Wu, J.; Lu, X.; Shen, Y.; Lu, Z. *Chem. Phys. Lett.* **1997**, *270*, 145. (d) Yanagi, H.; Chen, S.; Lee, P. A.; Nebesny, K. W.; Armstrong, N. R.; Fujishima, A. *J. Phys. Chem.* **1996**, *100*, 5447. (e) Deng, H.; Lu, Z.; Mao, H.; Xu, H. *Chem. Phys.* **1997**, *221*, 323.

(8) Nazeeruddin, M. K.; Humphry-Baker, R.; Grätzel, M.; Wöhrle, D.; Schnurpfeil, G.; Schneider, G.; Hirth, A.; Trombach, N. *J. Porphyrins Phthalocyanines* **1999**, *3*, 230.

(9) He, J.; Hagfeldt, A.; Lindquist, S.-E.; Grennberg, H.; Korodi, F.; Sun, L.; Åkermark, B. *Langmuir* **2001**, *17*, 2743.

(10) (a) Yachandra, V. K.; DeRose, V. J.; Latimer, M. J.; Mukerji, I.; Sauer, K.; Klein, M. P. *Science* **1993**, *260*, 675. (b) Tommos, C.; Tang, X.; Warncke, K.; Hoganson, C. W.; Styring, S.; McCracken, J.; Diner, B. A.; Babcock, G. T. *J. Am. Chem. Soc.* **1995**, *117*, 10325.

groups into phthalocyanine is to transfer an electron from tyrosine to the oxidized ZnPc, thereby preventing back-electron transfer. The performance of a sandwich solar cell based on ZnPcTyr-coated nanostructured TiO$_2$ electrodes prepared by different methods was compared with those based on ZnPcGly–TiO$_2$ electrodes. The relationship between solar cell performance and the extent of surface aggregation was investigated. The effects on solar cell performance of TBP in the electrolyte and of some additives in the dye solution for preparing dye-sensitized TiO$_2$ electrode were demonstrated. Furthermore, to explain the lower efficiency of a solar cell based on phthalocyanine compared to that based on the RuN3 dye, electron injection and recombination kinetics of ZnPcTyr-sensitized TiO$_2$ thin film were investigated by femtosecond pump–probe spectroscopy. The results were compared to the results obtained with RuN3-sensitized TiO$_2$ thin film.

Experimental Section

1. Synthesis. Materials and Structural Assignments. Starting materials, except for 3,4-dicyanobenzoyl chloride, were purchased from Lancaster. Crude acid chloride (3,4-dicyanobenzoyl chloride) was synthesized by refluxing 3,4-dicyanobenzoic acid[11] in thionyl chloride and chloroform, followed by evaporation and used immediately without further purification.

Melting points were measured on a Gallenkamp melting point apparatus and are uncorrected. Thin-layer chromatography (TLC) and column chromatography were performed by using silica gel adsorbent (Kieselgel F$_{254}$ and Kieselgel 60, 0.040–0.063 mm, respectively). Nuclear magnetic resonance (NMR) spectra were recorded on a Bruker AM 400 or Varian AS 400 instrument. The splitting of the signal is described as singlets (s), doublets (d), triplets (t), quartets (q), multiplets (m), or broad (br). MALDI-TOF MS investigations were carried out using a BRUKER BIFLEX III instrument in reflector mode, and 3,5-dimethoxy-4-hydroxy-trans-cinnamic acid (sinapinic acid) was used as a matrix in all cases.

4-Carboxy(*N*-tyrosine ethyl ester)phthalonitrile (1a). Crude acid chloride (ca. 10 mmol) was dissolved in acetonitrile (10 mL) and added dropwise to the mixture of tyrosine ethyl ester (2.45 g, 10 mmol), triethylamine (3.03 g, 40 mmol), and 10 mL of acetonitrile at 0–5 °C while stirring and cooling with ice–water bath during 20 min. The reaction mixture was stirred at the same temperature for an additional 10 min, and then 20 mL of water was added and extracted with dichloromethane (20 mL × 3). The organic phases were dried over sodium carbonate and then evaporated. The residue was purified by column chromatography using chloroform/methanol (95/5, v/v) as an eluent. Yield: 1.9 g (52%). Mp: 122–124 °C. ^{1}H NMR (CDCl$_3$) δ (ppm): 1.34 (t, 3H, J = 7.1 Hz, CH$_3$), 3.20 (m, 2H, CH$_2$), 4.27 (q, 2H, J = 7.1 Hz, CH$_2$), 5.01 (m, 1H, CH), 6.72 (d, 2H, J = 8.4 Hz, Ar (Tyr-3, 5)-H), 6.95 (d, 2H, J = 8.4 Hz, Ar(Tyr-2,6)-H), 7.88 (d, 1H, J = 8.1 Hz, Ar(nitrile-6)-H), 8.05 (dd, 1H, J_1=8.1 Hz, J_2=1.5 Hz, Ar-(nitrile-5)-H), 8.16 (d, 1H, J = 1.5 Hz, Ar(nitrile-3)-H).

2,9,16,23-Tetra[1-(*n*-butoxycarbonyl)-2-(4-hydroxyphenyl)eth-ylaminocarbonyl]phthalocyaninato Zinc(II) (2a). The mixture of **1a** (0.726 g, 2 mmol), DBU (0.456 g, 3 mmol), zinc(II) acetate dihydrate (0.11 g, 0.5 mmol), and butanol (10 mL) was refluxed for 1 h. After cooling to room temperature, 10 mL of diethyl ether was added and the mixture stirred for an additional 2 h. The precipitate was collected and washed by diethyl ether (3×). The crude product was purified by column chromatography eluted with a chloroform/ethanol (9/1, v/v) solution to get 292 mg (36%) of the title compound. ^{1}H NMR (DMSO-d_6) δ (ppm): 1.00 (t, 12H, J = 6.7 Hz, 4 × CH$_3$), 1.45 (m, 8H, 4 × CH$_2$), 1.70 (m, 8H, 4 × CH$_2$), 3.36 (br, 8H, 4 × CH$_2$), 4.25 (m, 8H,

4 × CH$_2$), 5.00 (br, 4H, 4 × CH), 6.87 (m, 8H, Ar(Tyr3,5)-H), 7.38 (m, 8H, Ar(Tyr2,6)-H), 8.60 (br, 4H, Ar(Pc)-H), 9.20 (br, 4H, Ar(Pc)-H), 9.32 (d, 4H, J = 10.8 Hz, NH), 9.62 (m, 4H, Ar(Pc)-H). MS: 1651.55 ([M + Na]$^+$), 1628.86 ([M]$^+$, calcd for C$_{88}$H$_{84}$N$_{12}$O$_{12}$Zn: 1628.54).

2,9,16,23-Tetra[1-carbonyl-2-(4-hydroxyphenyl)ethylaminocar-boxyl]phthalocyaninato Zinc(II) (ZnPcTyr). The mixture of **2a** (0.163 g, 0.1 mmol) and 5 M aqueous sodium hydroxide solution (0.2 mL, 1 mmol) was refluxed in 10 mL of acetone for 1 h. After cooling to room temperature, the precipitate was collected and washed with acetone. This sodium salt was dissolved in water (10 mL) and then 1 mL of 1 M aqueous hydrochloric acid solution was added to precipitate the product, which was collected and washed with water and diethyl ether to get 82 mg (59%) of the title compound. ^{1}H NMR (DMSO-d_6) δ (ppm): 3.39 (br, 8H, 4 × CH$_2$), 4.90 (br, 4H, 4 × CH), 6.82 (m, 8H, Ar (Tyr3, 5)-H), 7.37 (m, 8H, Ar(Tyr2,6)-H), 8.71 (br, 4H, Ar(Pc)-H), 9.26 (br, 4H, Ar(Pc)-H), 9.50 (br, 4H, NH), 9.94 (br, 4H, Ar(Pc)-H). MS: 1405.39 ([M]$^+$, calcd for C$_{72}$H$_{53}$N$_{12}$O$_{12}$Zn: 1405.29).

4-Carbonyl(*N*-glycine ethyl ester)phthalonitrile (1b). Crude acid chloride (ca. 10 mmol) was dissolved into acetonitrile (10 mL) and added dropwise to the mixture of glycine ethyl ester hydrochloride (1.4 g, 10 mmol), triethylamine (4.04 g, 40 mmol), and 10 mL of acetonitrile at 0–5 °C while stirring and cooling with ice–water bath during 30 min. The reaction mixture was stirred at the same temperature for an additional 10 min and then 20 mL of water was added and the solution extracted with chloroform (20 mL × 3). The organic phases were dried over sodium carbonate and then the solution was evaporated. The residue was purified by column chromatography eluting with a chloroform/methanol (95/5, v/v) solution to give 2.0 g (78%) of the title compound. Mp: 124–126 °C. ^{1}H NMR (CDCl$_3$) δ (ppm): 1.31 (t, 3H, J = 6.8 Hz, CH$_3$), 4.21–4.30 (m, 4H, CH$_2$ + CH$_2$), 7.04 (br, 1H, NH), 7.92(d, 1H, J = 8.1 Hz, Ar(6)-H), 8.16 (dd, 1H, J_1=8.1 Hz, J_2 =1.5 Hz, Ar(5)-H), 8.27 (d, 1H, J = 1.5 Hz, Ar(3)-H).

2,9,16,23-Tetra(*n*-butoxycarbonylmethylaminocarbonyl)-phthalocyaninato Zinc(II) (2b). The mixture of **1b** (0.77 g, 3 mmol), 1,8-diazabicyclo[5.4.0]undec-7-ene (DBU, 0.684 g, 4.5 mmol), zinc acetate dihydrate (0.165 g, 0.75 mmol), and butanol (15 mL) was refluxed for 1 h. After cooling to room temperature, hexane (45 mL) was added dropwise, and the reaction mixture was stirred for 2 h. The precipitate was collected, washed with diethyl ether (3×), and then dried. The crude product was subjected to column chromatography and eluted with a chloroform/ethanol (9/1, v/v) solution. The major fraction was collected, dried, and then washed with ether to afford pure **2b** at a yield of 304 mg (34%). ^{1}H NMR (DMSO-d_6) δ (ppm): 1.06 (t, 12H, J = 6.6 Hz, 4 × CH$_3$), 1.57 (m, 8H, 4 × CH$_2$), 1.80 (m, 8H, 4 × CH$_2$), 4.34 (t, 8H, J = 6.0 Hz, 4 × CH$_2$), 4.46 (s, 8H, 4 × CH$_2$), 8.66 (m, 4H, Ar–H), 8.98 (m, 4H, Ar–H). 9.48 (m, 4H, NH). 9.64 (m, 4H, Ar–H). ^{13}C NMR (DMSO-d_6) δ (ppm): 14.66, 19.70, 31.34, 42.86, 65.22, 122.26, 122.75, 129.10, 135.14, 137.67, 139.76, 151.89, 152.32, 167.87, 170.99. MS: 1205.45 ([M+H]$^+$, calcd for C$_{60}$H$_{61}$N$_{12}$O$_{12}$Zn: 1205.38).

2,9,16,23-Tetra(carbonylmethylaminocarboxyl)phthalo-cyaninato zinc(II) (ZnPcGly). The mixture of **2b** (120 mg, 0.1 mmol) and a 5 M aqueous sodium hydroxide solution (0.2 mL, 1 mmol) was refluxed in 10 mL of acetone for 1 h. After cooling to room temperature the precipitate was collected and washed with acetone. This sodium salt was dissolved in water (10 mL) and then 1 mL of 1 M aqueous hydrochloric acid solution was added to precipitate the product. The precipitate was collected and washed with water and diethyl ether. Yield: 87 mg (89%). ^{1}H NMR (DMSO-d_6) δ (ppm): 4.29 (s, 8H, 4 × CH$_2$), 8.74 (br, 4H, Ar–H), 9.38 (br, 4H, Ar–H), 9.64 (br, 4H, 4 × NH), 9.87 (br, 4H, Ar–H). ^{13}C NMR (DMSO-d_6) δ (ppm): 42.69, 122.23, 123.00, 129.35, 135.53, 138.56, 140.63, 153.31, 154.24, 167.69, 172.28. MS: 981.21 ([M + H]$^+$, calcd for C$_{44}$H$_{29}$N$_{12}$O$_{12}$-Zn: 981.13).

(11) George, R.; Snow, A. W. *J. Heterocycl. Chem.* **1995**, *32*, 495.

2. Electrochemical Measurements. The electrochemical experiments were performed at room temperature. A conventional three-electrode cell with separate compartments for counter and reference electrodes was employed in these experiments. A 3-mm glassy carbon disk acted as the working electrode, a nonaqueous Ag/Ag$^+$ electrode (10 mM AgNO$_3$ in acetonitrile) as the reference at a potential of 0.30 V vs SCE,[12] and a platinum wire as the counter electrode. The glassy carbon electrode was polished with Al$_2$O$_3$ paste and cleaned thoroughly in an ultrasonic water bath before each measurement. The electrolyte was 0.1 M tetrabutylammonium hexafluorophosphate (TBAPF$_6$) in dry acetonitrile/dimethyl sulfoxide (DMSO) (7/1, v/v). The concentration of the dyes in the electrolyte was ~0.5 mM. The potentiostat was an Autolab μII interfaced to a personal computer for data acquisition and instrument control.

3. Film Preparations and Dye-Coating. Colloidal TiO$_2$ paste (Ti−Nanoxide T) was purchased from Solaronix SA. According to the supplier's specification, the particle size of TiO$_2$ is ca. 13 nm and the paste is well-suited for preparation of transparent photoelectrodes for dye-sensitized solar cells. For obtaining a porous film of uniform thickness the following procedure was used. The colloidal TiO$_2$ suspension was spread onto transparent conducting glass sheets (Libbey Owens Ford, fluorine-doped SnO$_2$ glass, sheet resistance 8 Ω/□) using Scotch tape as a spacer. A thin film was obtained by raking off the excess of suspension with a glass rod. After removing the tape and air-drying, the sample was sintered in air at 450 °C for 30 min to form a transparent TiO$_2$ film electrode. This procedure was repeated two more times to obtain a thicker film. The thickness of the film, recorded by Dektak3 Surface Profile Measuring System, was about 7.6 μm. For femtosecond pump−probe measurements a ~2 μm thick nanostructured TiO$_2$ film was prepared on a ~60−80 μm microscope cover slip, according to the above-mentioned process.

Dye-coating of the TiO$_2$ film was carried out by soaking the film in the dye solution immediately after the high-temperature annealing and while it was still warm (~80 °C). ZnPcGly- and ZnPcTyr-sensitized TiO$_2$ film electrodes (denoted ZnPcGly−TiO$_2$ and ZnPcTyr−TiO$_2$) were prepared by dipping the TiO$_2$ films into a 5.0 × 10^{-5} M ZnPcGly− or ZnPcTyr−ethanol solution (containing 3% (v/v) DMSO for ZnPcGly) for 10 h, followed by rinsing with ethanol several times. To decrease dye aggregation on the semiconductor surface, 10 mmol cheno and 7% (v/v) TBP were added to the above dye solutions and the dye-sensitized TiO$_2$ film electrodes were obtained by dipping the TiO$_2$ films into the dye solutions with additives for 15 h and rinsing with ethanol immediately after withdrawal from the dye solutions. Sensitized electrodes prepared from dye solutions with additives are denoted (ZnPcGly−TiO$_2$)$_{add}$ and (ZnPcTyr−TiO$_2$)$_{add}$. Dye-coating of the TiO$_2$ film for pump−probe measurements was performed by immersing the film into the above ZnPcTyr−ethanol solution with additives for 10 h. The film was rinsed with ethanol, dried at room temperature, covered by acetonitrile and another microscope slip, and finally sealed. Steady-state absorption spectra of the dye-sensitized TiO$_2$ films in acetonitrile were recorded before and after laser experiments to ensure that no degradation or modification of the samples had occurred in sample preparation or during measurements. The optical density of the sample was ~0.65 at the excitation wavelength of 700 nm. All the dye-sensitized electrodes were stored in ethanol and kept in the dark before all measurements.

4. Optical and Photoelectric Measurements. Absorption spectra of the dye-sensitized TiO$_2$ electrodes were recorded on a JASCO V530 UV/vis spectrophotometer with a bare TiO$_2$ film as a reference. These measurements were carried out for dry film electrodes, and no corrections were made for optical effects due to the presence of the electrolyte. Photocurrent action spectra and photocurrent-photovoltage characteristics of the dye-sensitized TiO$_2$ electrodes were measured with

sandwich-type cells. The working electrode of the dye-sensitized TiO$_2$ film on conducting glass was squeezed together with a platinized conducting glass using a spring and illuminated from the substrate side. The electrolyte, typically 0.5 M LiI/0.05 M I$_2$ in propylene carbonate, was attracted into the cavities of the dye-sensitized TiO$_2$ electrode by capillary forces. A 450 W xenon lamp with a monochromator was used as light source for the photocurrent action spectra measurements. The cell was operated in the short-circuit mode. The IPCE values were determined at 10 nm intervals between 400 and 800 nm. The IPCE was then calculated according to the following equation:

$$\text{IPCE} = \frac{1240 i_{ph}[\mu A]}{P[\mu W]\lambda[nm]} \tag{1}$$

where i_{ph} and P are the photocurrent and power of the incident radiation per unit area and λ is the wavelength of the monochromatic light. No corrections were made for absorption and reflection in the substrate.

A 1000 W xenon lamp sun-simulator with a 10 cm water filter was used as a light source for the photocurrent−photovoltage characteristics. The light intensity was measured by a pyranometer (Kipp & Zonen CM 11). The active electrode area was typically 0.25 cm^2. The fill factor is defined by

$$\text{FF} = \frac{J_{Ph(max)} U_{Ph(max)}}{J_{SC} U_{OC}} \tag{2}$$

where $J_{Ph(max)}$ and $U_{Ph(max)}$ are the photocurrent and photovoltage for maximum power output and J_{SC} and U_{OC} are the short-circuit photo-current and open-circuit photovoltage. The overall conversion efficiency (η) is defined by the following equation:

$$\eta = \frac{J_{SC} U_{OC} \text{FF}}{P_{in}} \tag{3}$$

Here P_{in} is the power of incident white light.

5. Femtosecond Spectrometer. The femtosecond spectrometer used here was based on a regeneratively amplified mode-locked Ti:sapphire laser system working at 5 kHz repetition rate in combination with an optical parametric amplifier (OPA).[13] A detailed description of this setup has been presented previously.[14] Excitation pulses with a typical energy of ~0.2 μJ at 700 nm was focused to a spot of ~400 μm diameter at the sample position. The excitation pulse intensity of ~10^{14} photon/cm^2 used was far from the saturation limit considering that the optical cross section of the dye is ~1.5 × 10^{-16} cm^{-2}. The probe and reference pulses were taken from a white-light continuum generated by a part of the amplified fundamental 800 nm laser beam, which was sent into a sapphire plate. In the region from 1200 to 2000 nm, another OPA was used to generate the probe light. The polarization of pump and probe beams was kept at the magic angle configuration in all experiments. For data acquisition, a monochromator and three photodiodes in a single shot detection system were used. Transient absorption kinetics at a definite wavelength was recorded by keeping the detection wavelength fixed and scanning the pump−probe delay time. The instrument response function of ~140−150 fs (fwhm), depending slightly on the probe wavelength, was determined by sum frequency cross correlation in a BBO crystal. The accurate zero-time delay at all measured wavelengths was independently determined by sum frequency cross-correlation measurements and the nonresonant "spike signal" in a 1 mm thick glass plate. Measured kinetics were analyzed with the deconvolution software Spectra Solve 2.01, LASTEK Pty. Ltd. 1997. All experiments were conducted at room temperature.

Results and Discussion

1. Synthesis. The desired phthalocyanine dyes, ZnPcTyr and ZnPcGly, were synthesized as outlined in Scheme 1, by using

(12) *Handbook of Analytical Chemistry*; Meites L., Ed.; Mcgrow Hill, New York, 1963.

(13) Chachisvilis, M.; Kühn, O.; Pullerits, T.; Sundström, V. *J. Phys. Chem. B* **1997**, *101*, 7275.

(14) Benkö, G.; Hilgendorff, M.; Yartsev, A. P.; Sundström, V. *J. Phys. Chem. B* **2001**, *105*, 967.

Scheme 1
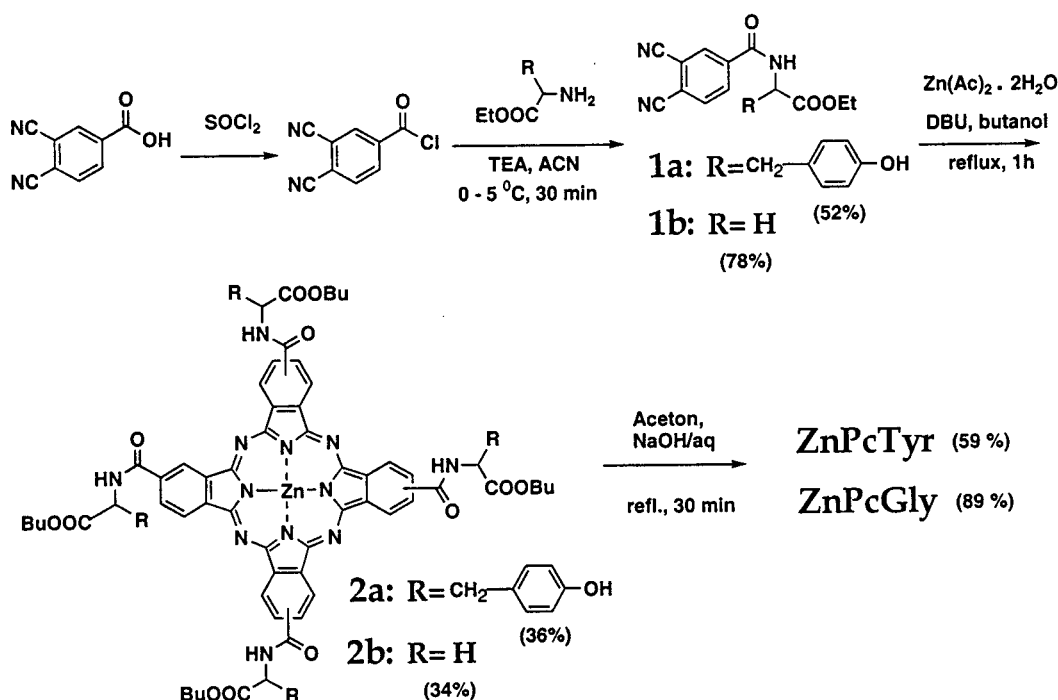
DBU as catalyst followed by saponification. The purpose of introducing amino acids as substituents is to provide carboxylic acids as attaching groups to the TiO$_2$ surface. Both ZnPcTyr and ZnPcGly were obtained in quite good yield. During the formation of the macrocycles, butoxy groups replaced ethoxy groups by transesterification with the solvent. The butyl esters (**2a** and **2b**) could be purified by means of column chromatography and eluted with a chloroform/ethanol solution. Furthermore, they were hydrolyzed successfully in both cases.

Phthalocyanines were characterized by NMR and mass spectrometry. MALDI-mass showed satisfactory results in all cases. ^{1}H NMR also agreed with the desired structure in all cases. Almost all the aromatic peaks became multiplets and/or broad after the formation of phthalocyanine rings, due to the existence of statistical isomers and possible aggregation. These observations supported the achievement of the designed structures.

2. Electrochemical Studies. Both ZnPcTyr and ZnPcGly were found to be soluble in an acetonitrile/DMSO (7/1, v/v) mixed solvent to a maximum concentration of ∼0.5−1 mM. The oxidation potentials were determined from half-wave potentials ($E_{1/2} = (E_{oxid} + E_{red})/2$) by cyclic voltammetry (CV) or peak potentials (E_p) by differential pulse voltammetry (DPV). Voltammograms were recorded at a glassy carbon electrode in the acetonitrile/DMSO solvent containing 0.1 M tetrabutylammonium hexafluorophosphate (TBAPF$_6$) that is redox passive in our scanning region (dashed lines in Figure 1). The cyclic voltammograms (CVs, dotted lines) and differential pulse voltammograms (DPVs, solid lines) of ZnPcGly and ZnPcTyr are shown in parts A and B of Figure 1, respectively. The cyclic voltammograms are not well-resolved and are partly distorted, presumably due to aggregation of the poorly soluble phthalocyanines. The separation between anodic and cathodic CV peaks is difficult to determine accurately, but the oxidations I and II appear to be reversible one-electron processes for both ZnPcGly and ZnPcTyr.[15] Reasonably well resolved voltammograms were

obtained by DPV, owing to smaller charging effects.[16] Relative voltammetric peak heights and DPV peak areas indicate that oxidation III of ZnPcTyr (Figure 1B) is a one-electron process, while the third oxidation of ZnPcGly (Figure 1A) seems to involve more than one electron. The reversible peaks I and II of ZnPcGly (Figure 1A) can be assigned to oxidations generating the π-cation radical and the dication.[17] The oxidation potentials are 0.17 V vs Ag/AgNO$_3$ (0.47 V vs SCE) and 0.36 V vs Ag/AgNO$_3$ (0.66 V vs SCE), respectively. The additional peaks (III and IV) observed at 0.72 and 0.96 V vs Ag/AgNO$_3$ or 1.02 and 1.26 V vs SCE, respectively, have not been reported before for zinc phthalocyanines and are not observed for ZnPcTyr (Figure 1B). From our present data, no assignment can be made for these peaks. In the case of ZnPcTyr (Figure 1B), three oxidations at 0.25, 0.40, and 0.55 V vs Ag/AgNO$_3$ or 0.55, 0.70, and 0.85 V vs SCE are observed. By comparison with the oxidation potentials of ZnPcGly, the first and second oxidation peak can be assigned to the oxidations of the marocycle of ZnPcTyr. The oxidation potentials of ZnPcTyr (0.55 and 0.70 V vs SCE) are more positive than those of ZnPcGly (0.47 and 0.66 V vs SCE), owing to the electron-withdrawing effect of the tyrosine group.[18] The third oxidation peak of ZnPcTyr is assigned to the oxidation of one of the tyrosines on the basis of a reported oxidation potential of 0.84 V vs SCE[19] for tyrosine in acetonitrile, which is in good agreement with the value of 0.85 V vs SCE observed with ZnPcTyr. It seems unlikely that the third peak of ZnPcTyr is due to the same oxidation process

(15) Kissinger, P. T.; Heineman, W. R. *J. Chem. Educ.* **1983**, *60*, 702.
(16) Bard, A. L.; Faulkner, L. R. *Electrochemical Methods: Fundamentals and Applications*; Wiley: New York, 1980.
(17) (a) Nyokong, T.; Gasyna, Z.; Stillman, M. J. *Inorg. Chem.* **1987**, *26*, 548. (b) Manivannan, V.; Nevin, W. A.; Leznoff, C. C.; Lever, A. B. P. *J. Coord. Chem.* **1988**, *19*, 139.
(18) Zhou, Y.; Wang, Z.; Wang, D.; Sugiura, K.; Sakata, Y. *J. Porphyrins Phthalocyanines* **2001**, *5*, 523.
(19) Sun, L.; Burkitt, M.; Tamm, M.; Ramond, M. K.; Abrahamsson, M.; LeGourriérec, D.; Frapart, Y.; Magnuson, A.; Kenéz, P. H.; Brandt, P.; Tran, A.; Hammarström, L.; Styring S.; Åkermark, B. *J. Am. Chem. Soc.* **1999**, *121*, 6834.
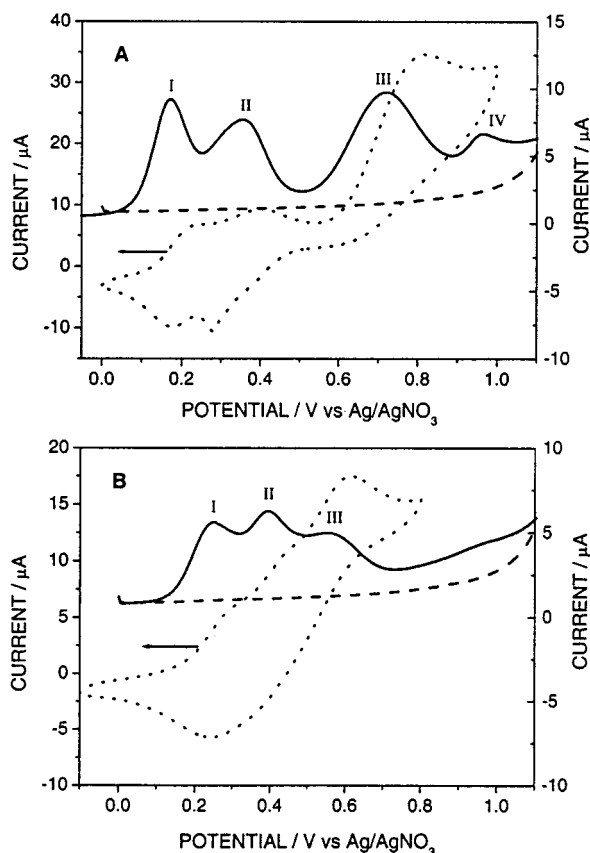
Figure 1. Differential pulse voltammograms (solid lines) and cyclic voltammograms (dotted lines) of ~0.5 mM ZnPcGly (A) and ZnPcTyr (B). Dry acetonitrile/DMSO (7/1, v/v) containing 0.1 M TBAPF$_6$ was used as supporting electrolyte. Dashed lines are the DPVs of 0.1M TBAPF$_6$ in dry acetonitrile/DMSO (7/1, v/v). I, II, III and IV represent the first, second, third, and fourth oxidations, respectively. Scans are initiated at −0.05 or 0 V versus Ag/AgNO$_3$ in positive direction at the rates of 50 mV/s. In the case of DPV, the modulation time is 50 ms, interval time 100 ms, step potential 5 mV, and modulation amplitude 25 mV. The solutions were purged with argon and stirred for over 15 min prior to the measurements. The solutions were kept under argon during the measurements.

that gives rise to the third peak of ZnPcGly, since the latter occurs at substantially higher potential (1.02 V vs SCE) and involves more than one electron. That the further oxidations of ZnPcGly (Figure 1A, peaks III and IV, 1.02 and 1.26 V vs SCE) are not observed with ZnPcTyr is probably due to the reactivity of the tyrosine radical formed from ZnPcTyr at 0.85 V vs SCE (Figure 1B, peak III).

With respect to dye-sensitization of large band-gap semiconductors, e.g. TiO$_2$, the first oxidation process is of interest. From the first oxidation potentials of ZnPcGly and ZnPcTyr and their 0−0 transition energy (E_{0-0}) of 1.82 eV assessed from the respective absorption and emission spectral data (not shown), the energy levels of the singlet excited states (LUMO) of ZnPcGly and ZnPcTyr were determined to be −1.35 and −1.27 V vs SCE, respectively, whereas the energy level of the conduction band edge of TiO$_2$ is ca. −0.74 V vs SCE.[3] This makes electron injection from the excited state of ZnPcGly or ZnPcTyr into the conduction band of TiO$_2$ thermodynamically possible. Furthermore, the HOMO levels of the dyes ($E_{ZnPcGly/ZnPcGly^+}$ and $E_{ZnPcTyr/ZnPcTyr^+}$) are lower than the energy level of the redox couple I$^-$/I$_3^-$ (0.2 V vs SCE[3]) in the electrolyte, enabling the dye regeneration by electron transfer from I$^-$.
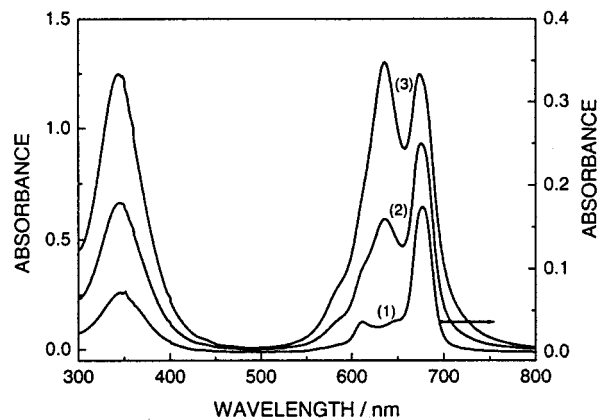
Figure 2. Absorption spectra of ZnPcTyr in ethanol at different concentrations. (1) 1.0×10^{-6} M; (2) 1.0×10^{-5} M, and (3) 2.0×10^{-5} M.

As mentioned in the Introduction, incorporating the redox-active tyrosine groups into phthalocyanine has the potential function of blocking back-electron transfer from the conduction band of TiO$_2$ to the oxidized sensitizer by electron transfer from tyrosine to the oxidized ZnPc. However, since the oxidation potential of tyrosine is more positive than that of the zinc phthalocyanine macrocycle, it is evident that this process is thermodynamically impossible.

3. Steady-State Spectroscopies. ZnPcGly is insoluble in pure ethanol. However, it is soluble in ethanol with the aid of DMSO (3%, v/v). In contrast, ZnPcTyr has an appreciable solubility in ethanol, suggesting that the tyrosine groups incorporated into the zinc phthalocyanine macrocycle are crucial for obtaining good solubility in ethanol. Figure 2 shows the absorption spectra of ZnPcTyr in ethanol at different concentrations. In dilute solution (curve 1) ZnPcTyr is present mainly as monomers, characterized by the sharp absorption bands in the Soret (350 nm) and in the Q-band region (680 nm).[20,21] On increasing the dye concentration (curve 2), a new absorption band at around 635 nm appears and becomes stronger compared to the 680-nm band (curve 3) with further increase of the dye concentration. This blue-shifted band with a maximum at 635 nm can be assigned as the characteristic Q-band of the ZnPcTyr face-to-face dimer or higher order aggregate (H-aggregate).[21,22] A similar behavior was also found for ZnPcGly in ethanol containing 3% (v/v) DMSO (not shown).

Absorption spectra of the dye-sensitized TiO$_2$ electrodes and a bare TiO$_2$ film are shown in Figure 3. Curves 1 and 2 are the absorption spectra of ZnPcTyr−TiO$_2$ and ZnPcGly−TiO$_2$ electrodes, respectively, prepared from their corresponding dye−ethanol solutions under identical conditions except that 3% (v/v) DMSO was added to the solution of ZnPcGly. Curves 3 and 4 are the absorption spectra of (ZnPcTyr−TiO$_2$)$_{add}$ and (ZnPcGly−TiO$_2$)$_{add}$ electrodes prepared under identical conditions (except for 3% (v/v) DMSO was added to in the ZnPcGly solution) from their corresponding dye−ethanol solutions with additives (10 mmol cheno and 7% (v/v) TBP). Curve 5 is the absorption spectrum of a bare TiO$_2$ film. It is interesting to see that adsorption of dye onto the TiO$_2$ film makes the film more

(20) *Phthalocyanine Materials*, Mckeown, N. B., Ed.; Cambridge University Press: Cambridge, 1998.
(21) Schlettwein, D.; Oekermann, T.; Yoshida, T.; Tochimoto, M.; Minoura, H. *J. Electroanal. Chem.* **2000**, *481*, 42.
(22) (a) Nevin, W. A.; Liu, W.; Lever, A. B. P. *Can. J. Chem.* **1987**, *65*, 855. (b) Snow, A. W.; Jarvis, N. L. *J. Am. Chem. Soc.* **1984**, *106*, 4706.
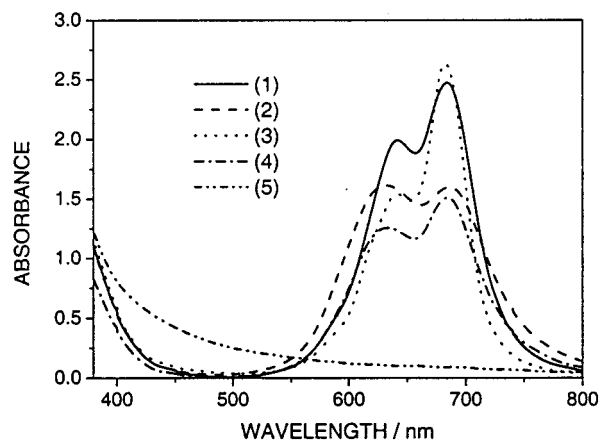
Figure 3. Absorption spectra of the dye-sensitized nanostructured TiO$_2$ film electrodes (1−4) referenced by a bare TiO$_2$ film and of a TiO$_2$ film (5) with conducting glass as a reference. (1) and (3) are the spectra of ZnPcTyr−TiO$_2$ and (ZnPcTyr−TiO$_2$)$_{add}$ electrodes prepared from ZnPcTyr solutions without and with additives. (2) and (4) are the spectra of ZnPcGly−TiO$_2$ and (ZnPcGly−TiO$_2$)$_{add}$ electrodes prepared from ZnPcGly solutions without and with additives.

Table 1. Optical Data of the Dye-Sensitized TiO$_2$ Electrodes and Photovoltaic Data of the Sandwich Solar Cells Based on These Electrodes

electrodes	A_a/A_m	IPCE/% (690 nm)	ϕ/% (690 nm)	J_{SC}/mA cm^2	U_{OC}/V	FF/%	η/%
ZnPcTyr−TiO$_2$	0.80	6.9	6.9	1.27	0.36	64	0.29
ZnPcGly−TiO$_2$	1.01	4.0	4.1	0.36	0.31	65	0.07
(ZnPcTyr−TiO$_2$)$_{add}$	0.59	24.2	24.3	2.25	0.36	67	0.54
(ZnPcGly−TiO$_2$)$_{add}$	0.83	5.5	5.7	0.61	0.32	68	0.13

transparent in the 400−500 nm region, indicating that the dye-sensitized TiO$_2$ electrodes have less light scattering than the bare electrodes in this spectral region. Each spectrum of the dye-sensitized TiO$_2$ electrode shows two Q-bands, one near the position of the monomer Q-band and the other near the position of the Q-band of the aggregate of the dye in solution (Figure 2). Each system is therefore characterized by adsorption to the TiO$_2$ surface of a mixture between monomers and aggregates. The two Q-bands of ZnPcTyr and the Q-band of the ZnPcGly monomer red-shift by ∼5 nm compared to the dyes in ethanol solution (Figure 2), indicating a strong interaction between the dyes and the semiconductor surface.[23] The Q-band of the ZnPcGly aggregate blue-shifts by ∼2 nm, which may be induced by a heavier surface aggregation of ZnPcGly compared to that of ZnPcTyr. To estimate the extent of surface aggregation of the above four dye-sensitized TiO$_2$ electrodes, the ratio of the absorbance at the aggregate band maximum (633 nm for ZnPcGly and 640 nm for ZnPcTyr) (A_a) and that of monomer (685 nm) (A_m) of each system was calculated (see Table 1). We can see that the A_a/A_m of the ZnPcTyr−TiO$_2$ electrode (0.80) is lower than that of the ZnPcGly−TiO$_2$ electrode (1.01), implying that the extent of surface aggregation for ZnPcTyr is less than that for ZnPcGly. It is conceivable that the presence of tyrosine groups in ZnPcTyr reduces the formation of dye H-aggregates on the TiO$_2$ surface because of steric effects. It was found[8] that addition of some chemicals, such as cheno and TBP, to the zinc phthalocyanine solution from which the dye-sensitized TiO$_2$ electrode was prepared significantly diminishes
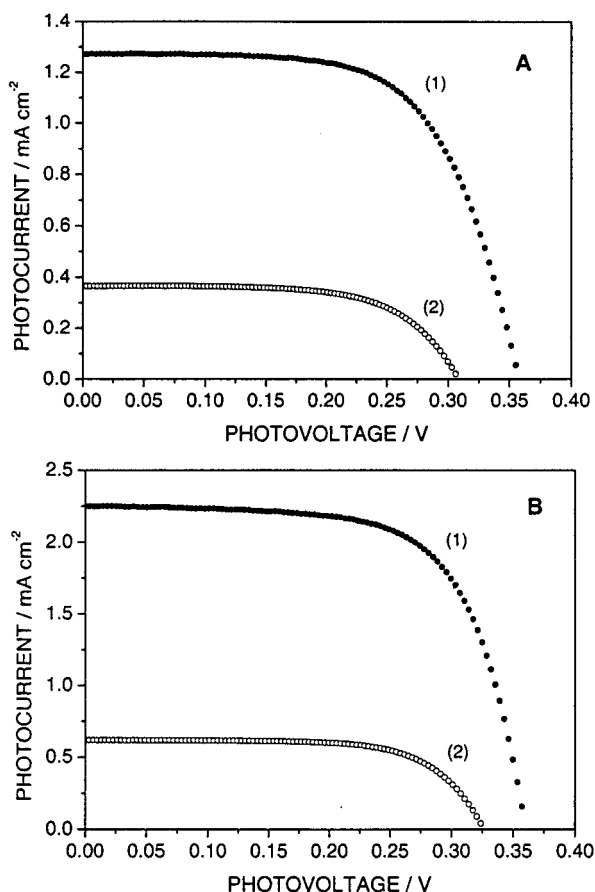
(23) Kamat, P. V. *Chem. Rev.* **1993**, *93*, 267.
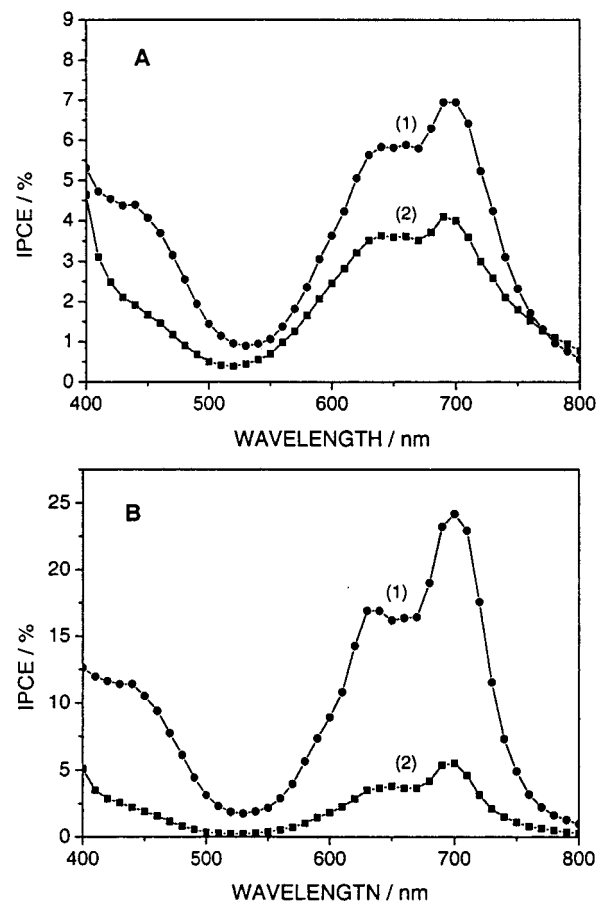
Figure 4. Photocurrent action spectra of sandwich solar cells based on the same ZnPcTyr−TiO$_2$ (1) and ZnPcGly−TiO$_2$ (2) electrodes (A), and (ZnPcTyr−TiO$_2$)$_{add}$ (1) and (ZnPcGly−TiO$_2$)$_{add}$ (2) electrodes (B) as those in Figure 3.

the surface aggregation of the sensitizer. The cheno molecules are expected to coadsorb with the dye molecules to avoid to some extent the dye aggregation on the semiconductor surface, while the TBP will coordinate to the axial position of the zinc phthalocyanine, preventing stacking of the dye molecules. It is seen from Figure 3 and Table 1 that the electrodes (ZnPcTyr−TiO$_2$)$_{add}$ and (ZnPcGly−TiO$_2$)$_{add}$ prepared from their corresponding dye solutions with these additives have less extent of surface aggregation than ZnPcTyr−TiO$_2$ and ZnPcGly−TiO$_2$, respectively. By addition of these additives, the A_a/A_m of the ZnPcTyr−TiO$_2$ electrode is decreased by 26% (from 0.80 to 0.59), while the A_a/A_m of ZnPcGly−TiO$_2$ electrode is reduced by 18% (from 1.01 to 0.83). The larger A_a/A_m decrease for the ZnPcTyr−TiO$_2$ electrode as compared to the ZnPcGly−TiO$_2$ electrode can also be explained by steric effects of tyrosine groups in ZnPcTyr.

4. Photovoltaic Studies. The four dye-sensitized TiO$_2$ electrodes were employed as working electrodes in sandwich solar cells, and the performance of the cells was characterized by spectral photocurrent responses and photocurrent−photovoltage characteristics. Figure 4a shows the photocurrent action spectra of solar cells with ZnPcTyr−TiO$_2$ and ZnPcGly−TiO$_2$ as working electrodes, while the photocurrent action spectra of the cells based on (ZnPcTyr−TiO$_2$)$_{add}$ and (ZnPcGly−TiO$_2$)$_{add}$ working electrodes are shown in Figure 4b. The photocurrent action spectra resemble the absorption spectra (Figure 3) except

Figure 5. Photocurrent−photovoltage characteristics of sandwich solar cells based on the same ZnPcTyr−TiO₂ (1) and ZnPcGly−TiO₂ (2) electrodes (A), and (ZnPcTyr−TiO₂)ₐ𝒹𝒹 (1) and (ZnPcGly−TiO₂)ₐ𝒹𝒹 (2) electrodes (B) as those in Figure 3. The light intensity was 100 mW/cm².

for a slight red-shift by ca. 5 nm. The highest IPCE values at 690 nm for each system are summarized in Table 1. Taking into consideration the different light-harvesting efficiencies of the various systems, the quantum efficiency (ϕ), defined as electrons measured in the external circuit per absorbed photon at a definite wavelength as in the following equation,[24] is determined to provide a appropriate comparison.

$$\phi = \frac{\text{IPCE}}{1 - R - T} \quad (4)$$

In eq 4, R and T are the reflectance and transmission of the electrodes, and R can be considered to be 0 because the dye-sensitized TiO₂ electrodes scatter little light (see Figure 3 and the text in section 3). The quantum efficiencies obtained at 690 nm are listed in Table 1. It should be noted that the quantum efficiency is very close to the IPCE value, because the absorptance $(1 - R - T)$ is close to 1 for all electrodes. Figure 5 shows the photocurrent−photovoltage characteristics of sandwich solar cells based on the four dye-sensitized TiO₂ electrodes illuminated by a sun simulator. The short-circuit photocurrent (J_{SC}), open-circuit photovoltage (U_{OC}), fill factor (FF), and overall conversion efficiency (η) for each system are also summarized in Table 1. We can see that all the IPCE, ϕ, and η for the ZnPcTyr−TiO₂ electrode are higher than those of the ZnPcGly−TiO₂ electrode. When comparing the dye-

(24) O'Regan, B.; Schwartz, D. T. *Chem. Mater.* **1995**, *7*, 1349.

sensitized TiO₂ electrodes prepared from their corresponding dye solutions with additives, it is seen that the IPCE, ϕ, and η values for the (ZnPcTyr−TiO₂)ₐ𝒹𝒹 electrode are also much higher than those of the (ZnPcGly−TiO₂)ₐ𝒹𝒹 electrode. Furthermore, the (ZnPcTyr−TiO₂)ₐ𝒹𝒹 and (ZnPcGly−TiO₂)ₐ𝒹𝒹 electrodes have higher IPCE, ϕ, and η values as compared to the corresponding electrodes prepared without additives to the dye solutions. By comparison to the absorption spectra of the dye-sensitized TiO₂ electrodes (Figure 3), these results indicate that surface aggregation of the phthalocyanines plays an important role in the performance of the solar cells. Reducing surface aggregation leads to a considerable increase in solar cell performance, which can be explained as suppression of quenching processes due to energy transfer[25] or charge-transfer reactions[26] between aggregated molecules and/or between molecules in the aggregates and monomers. Due to the steric effects of the tyrosine groups in ZnPcTyr, this sensitizer has a lower degree of aggregation on the surface compared to ZnPcGly (Figure 3 and Table 1), which leads to a much better performance of solar cells based on ZnPcTyr-sensitized TiO₂ electrodes. Addition of cheno and TBP to the dye solutions decreases the surface aggregation and enhances significantly the solar cell performance, especially for ZnPcTyr. The (ZnPcTyr−TiO₂)ₐ𝒹𝒹 electrode has the highest IPCE of 24.2% at 690 nm, corresponding to a ϕ of 24.3%, J_{SC} of 2.25 mA/cm², U_{OC} of 360 mV, and FF of 67%, giving a η of 0.54%. This is one of the highest efficiencies reported for a photovoltaic device based on phthalocyanine.

5. Effect of TBP in the Electrolyte. It has been demonstrated previously that pretreatment of dye-sensitized nanostructured TiO₂ electrodes with TBP[2] or adding TBP in the electrolyte[27] enhances dramatically the open-circuit photovoltage without apparent loss in short-circuit photocurrent. The general explanation is that the adsorption of TBP on the free area of the TiO₂ electrode exposed to redox electrolyte suppresses the dark current, arising from the triiodide reduction by conduction band electrons at the semiconductor electrolyte junction (eq 5).

$$2\mathrm{e}_{cb}^{-}(\mathrm{TiO_2}) + \mathrm{I_3}^{-} \xrightarrow{k_{et}[\mathrm{I_3}^{-}]} 3\mathrm{I}^{-} \quad (5)$$
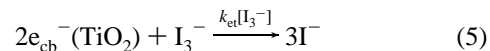
For regenerative photoelectrochemical systems, eq 6 holds:[2]

$$U_{OC} = \left(\frac{kT}{\mathrm{e}}\right)\ln\left(\frac{I_{inj}}{n_{cb}k_{et}[\mathrm{I_3}^{-}]}\right) \quad (6)$$

where k and T are the Boltzmann constant and absolute temperature, I_{inj} is the flux of charge resulting from electron injection from the sensitizing dye, n_{cb} is the concentration of electrons at the TiO₂ surface, and k_{et} is the rate constant for triiodide reduction by conduction band electrons. A decrease of the rate constant for triiodide reduction should result in an increase in the open-circuit photovoltage. More recently, Hag-

(25) (a) Schneider, G.; Wöhrle, D.; Spiller, W.; Stark, J.; Schulz-Ekloff, G. *Photochem. Photobiol.* **1994**, *60*, 333. (b) Spiller, W.; Kliesch, H.; Wöhrle, D.; Hackbarth, S.; Roeder, B. *J. Porphyrins. Phthalocyanines* **1998**, *2*, 145.
(26) (a) Klessinger, M.; Michl, J. *Excited States and Photochemistry of Organic Molecules;* VCH: New York, 1995; (b) Rodgers, M. A. J. *Photosensitization*; Moreno, G., Pottier, R. H., Truscott, T. G., Eds.; Springer: Berlin, 1988.
(27) (a) Gómez, M. M.; Lu, J.; Solis, J. L.; Olsson, E.; Hagfeldt, A.; Granqvist, C. G. *J. Phys. Chem. B* **2000**, *104*, 8712. (b) Park, N.-G.; van de Lagemaat, J.; Frank, A. J. *J. Phys. Chem. B* **2000**, *104*, 8989. (c) Sayama, K.; Hara, K.; Mori, N.; Satsuki, M.; Suga, S.; Tsukagoshi, S.; Abe, Y.; Sugihara, H.; Arakawa, H. *Chem. Commun.* **2000**, 1173.
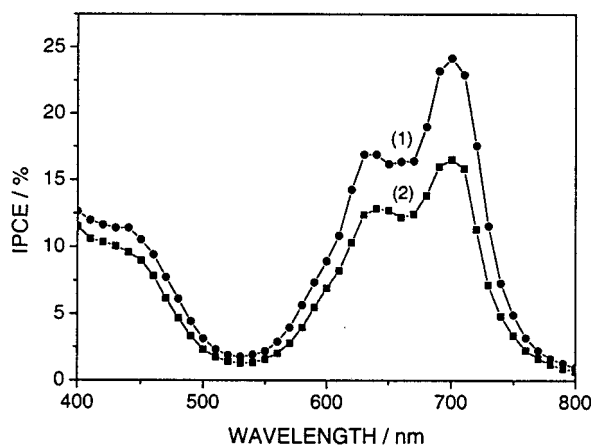
Figure 6. Photocurrent action spectra of sandwich solar cells based on a (ZnPcTyr−TiO$_2$)$_{add}$ film electrode using 0.5 M LiI/0.05 M I$_2$ in propylene carbonate (1) and 0.5 M LiI/0.05 M I$_2$/0.2 M TBP in propylene carbonate (2) as electrolyte.
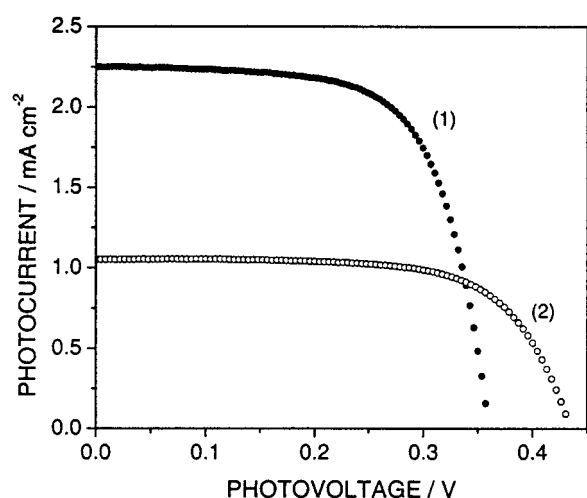
Figure 7. Photocurrent−photovoltage characteristics of sandwich solar cells based on the same (ZnPcTyr−TiO$_2$)$_{add}$ film electrode as that in Figure 6 using 0.5 M LiI/0.05 M I$_2$ in propylene carbonate (1) and 0.5 M LiI/0.05 M I$_2$/0.2 M TBP in propylene carbonate (2) as electrolyte.

feldt and co-workers[28] demonstrated another function of TBP added in the electrolyte in a RuN3-sensitized nanostructured TiO$_2$ solar cell: suppression of the loss of thiocyanato (SCN$^-$) groups from the dye so as to improve the stability of the cell. To further improve the performance of the solar cells based on our phthalocyanine dyes, TBP was added to the I$^-$/I$_3^-$ redox electrolyte. Figure 6 shows the photocurrent action spectra of the sandwich solar cells based on a ZnPcTyr−TiO$_2$ electrode using 0.5 M LiI/0.05 M I$_2$ (curve 1) or 0.5 M LiI/0.05 M I$_2$/0.2 M TBP (curve 2) in propylene carbonate as the electrolyte. The photocurrent−photovoltage characteristics of the same cells are shown in Figure 7. We can see that the open-circuit photovoltage increases by ∼20%, but the short-circuit photocurrent decreases by ∼50% when adding TBP to the electrolyte; overall, this leads to a decrease in the conversion efficiency from 0.54% to 0.31%. The IPCE values also decrease, for example by ∼35% at 690 nm. Similar behavior was also found for the cells based on the other three phthalocyanine-sensitized TiO$_2$ electrodes (not shown). The origin of the decreased short-circuit photocurrent

and IPCE with addition of TBP to the electrolyte is not known at present.

6. Ultrafast Spectroscopic Measurements. As demonstrated above, the best solar cell presented here is based on a (ZnPcTyr−TiO$_2$)$_{add}$ electrode. It has a quantum efficiency of ∼24% at 690 nm and an overall conversion efficiency of 0.54%. Aiming for a good performance, one can compare the (ZnPc-Tyr−TiO$_2$)$_{add}$ and RuN3-based cells, since the solar cell based on RuN3-sensitized TiO$_2$ shows a quantum efficiency of ∼100% and an overall conversion efficiency of ∼10%.[4a,d] It is well-known that besides other important properties, the several orders of magnitude difference between the time constants of electron injection (ranging from ∼50 fs to tens of picoseconds[29]) and recombination (on the nanosecond to millisecond time scales[30]), make the RuN3−TiO$_2$ system one of the most efficient light-to-energy converters available for DSSC. The apparent difference between the two DSSCs naturally raises the question whether the relatively low performance of (ZnPcTyr−TiO$_2$)$_{add}$ DSSC may be caused by either slow electron injection or/and fast charge recombination. It is important to point out that in DSSC the overall conversion yield is the result of a kinetic competition between reactions of the oxidized dye molecules with conduction band electrons and redox species. It is crucial that the recombination with conduction band electrons should be slower than interception of the dye cation by a redox mediator. In RuN3-based solar cells, this later process was shown to take place within about 10 ns,[31] although there are systems where part of the oxidized dye reduction occurs already on the tens of picoseconds time scale.[14]

For clarifying the issue of whether electron injection or recombination controls the overall conversion yield in our solar cell, the kinetics of a ZnPcTyr-sensitized TiO$_2$ thin film was studied by femtosecond pump−probe spectroscopy, and the results were compared with those obtained for a RuN3-coated TiO$_2$ thin film. Here, only a limited number of kinetics monitoring the interfacial electron-transfer reactions in our sample is presented. The detailed femtosecond transient absorption study focusing on TiO$_2$ film sensitized by ZnPcTyr and containing acetonitrile as solvent will be published elsewhere.[32]

In transient absorption spectroscopy, the electron injection process can be monitored by the formation of the electron-transfer products, the injected electrons in the conduction band of the semiconductor (e$^-_{TiO_2}$), or the oxidized dye molecule (ZnPcTyr$^+$). The decay of the electron-transfer products and the recovery of the ground-state bleach (GSR) are indicative of the charge recombination reaction. For the ZnPcTyr-sensitized TiO$_2$ thin film, we have chosen an excitation wavelength of 700 nm to ensure a selective excitation of the monomers (see curve 3 in Figure 3). Figure 8 shows the transient absorption kinetics recorded at 1800 nm. On the basis of the extinction coefficient of conduction band electrons in the near-IR,[33] the rise of the weak induced absorption is assigned to the arrival

(28) Greijer, H.; Lindgren J.; Hagfeldt, A. *J. Phys. Chem. B* **2001**, *105*, 6314.

(29) Benkö, G.; Kallioinen, J.; Korppi-Tommola, J. E.; Yartsev, A. P.; Sundström, V. *J. Am. Chem. Soc.* **2002**, *124*, 489. and references therein.
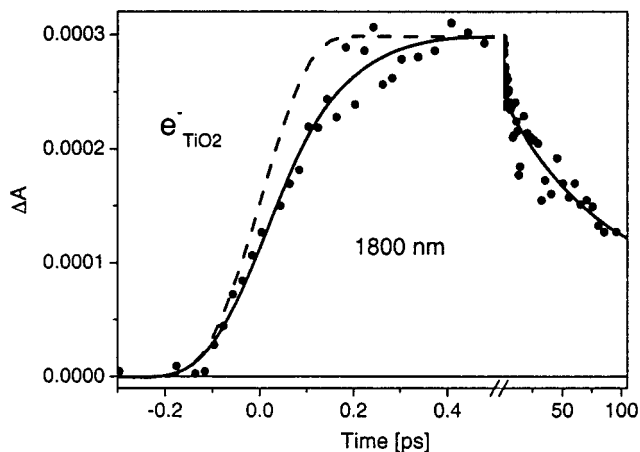(30) Haque, S. A.; Tachibana, Y.; Willis, R. L.; Moser, J. E.; Grätzel, M.; Klug, D. R.; Durrant, J. R. *J. Phys. Chem. B* **2000**, *104*, 538.
(31) Grätzel, M.; Moser, J.-E. Solar Energy Conversion. In *Electron Transfer in Chemistry*; Balzani, V., Gould, I., Eds.; Wiley-VCH: Weinheim, 2001; Vol. V, p 589, and references therein.
(32) Benkö, G.; He, J.; Yartsev, A. P.; Polívka, T.; Sundström, V. To be published.
(33) (a) van't Spijker, H.; O'Regan, B.; Goossens, A. *J. Phys. Chem. B* **2001**, *105*, 7220. (b) Benkö, G.; Yartsev, A. P.; Sundström, V. Unpublished results.
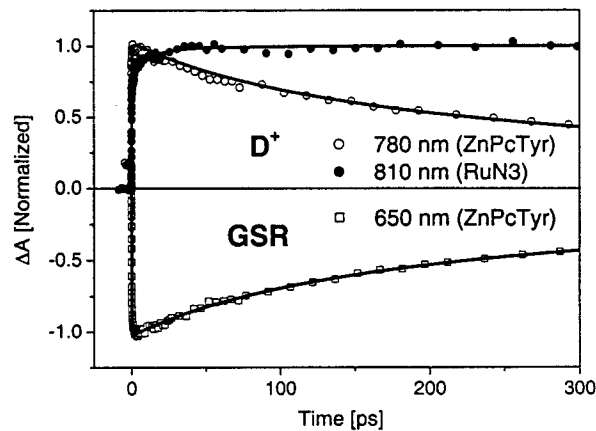
Figure 8. Rise kinetics of conduction band electrons in a ZnPcTyr−TiO₂ thin film at 1800 nm induced by a ∼100 fs pulse at 700 nm. Solid circles are experimental data points and the dashed line represents the instrument response function, while the solid line is a kinetic fit. See the text for details.

Figure 9. Transient absorption kinetics of the ZnPcTyr-sensitized TiO₂ thin film at 780 nm (oxidized dye) and 650 nm (GSR). For comparison, kinetics of the oxidized dye in the RuN3-sensitized TiO₂ film in acetonitrile is shown. The kinetics for RuN3 was taken from our previous report.[36] Symbols are experimental data points, while the solid curves are fits. See the text for details.

of electrons in the conduction band of the TiO₂ and shows that the overall injection is over in ∼500 fs. The best fit to the experimental data yields the following time constants and amplitudes (in parentheses)─rise within the laser pulse (25%), delayed rise 160 fs (75%)─and decay─0.6 ps (40%), 50 ps (40%), >1 ns (20%). The pulse-limited rise may be due to either a very fast electron injection, which we are not capable of resolving with our spectrometer, and/or excited state absorption of the phthalocyanine present at this wavelength. The main component (160 fs) we assign solely to electron injection. Kinetics recorded at around 780 nm (data not shown) show the formation of the oxidized dye[34,35] with very similar rise time as for the conduction band electrons.

As pointed out above, the decay of e⁻_{TiO₂}, ZnPcTyr⁺ signals, and GSR measured at 1800, 780, and 650 nm, respectively, can be used to characterize the recombination process in the ZnPcTyr-sensitized TiO₂ film. The normalized kinetics of the two later signals is shown in Figure 9. The decays can be fitted with the identical time constants of 50 ps (12%), 250 ps (65%), and >1 ns (23%), which suggests a widely distributed recombination rate ranging from a few tens of picoseconds up to longer times. The fit to the decay of the electron absorption signal (see Figure 8) also contains a subpicosecond time constant, which is attributed to electron thermalization and trapping dynamics within the TiO₂, a process that takes place after injection.[31]

Comparing electron injection and recombination kinetics in ZnPcTyr and RuN3-sensitized TiO₂ films (comparison shown in Figure 9), one can see that electron injection for the former system proceeds in ∼500 fs (see Figure 8), while for the latter system it is completed only after ∼100 ps.[29] Therefore, ZnPcTyr is slightly better than RuN3 from the electron injection point of view, and the charge injection does not control the conversion yield. However, the recombination in ZnPCTyr−TiO₂ is considerably faster than it is in RuN3−TiO₂. In fact, more

than half of the injected electrons recombine with the oxidized dye in 300 ps (Figure 9). For RuN3−TiO₂, there is no recombination in 300 ps, as recombination occurs at much longer times.[30] The comparison of the two systems allows us to conclude that the most important condition necessary for efficient light-to-current conversion (very fast injection combined with slow recombination) is not established in the ZnPcTyr−TiO₂ electrode. The next important condition (ZnPcTyr⁺ reaction with I⁻) was not studied in the present work. Since recombination is very fast (a major part of it occurs on the picosecond time scale), the original state of the dye will be restored mainly by conduction band electrons, before the reaction between oxidized dye and iodide could take place. As a result, the very fast electron recombination probably leads to the low quantum efficiency and low overall conversion efficiency of the ZnPcTyr-based DSSC.

Conclusions and Perspectives

The synthesis of a modified zinc phthalocyanine with tyrosine substituents (ZnPcTyr) and its reference, glycine-substituted zinc phthalocyanine (ZnPcGly), is described. Incorporation of tyrosine groups makes the dye ethanol-soluble and decreases considerably surface aggregation of the sensitizer due to steric effects and as a result improves the solar cell performance. Addition of cheno and TBP to the sensitizing dye solutions diminishes surface aggregation of the sensitizers, especially for ZnPcTyr, and therefore enhances significantly the solar cell performance. Since the oxidation potential of tyrosine is more positive than that of the zinc phthalocyanine macrocycle, electron transfer from tyrosine to the oxidized phthalocyanine is thermodynamically impossible and therefore not a possible route to block back-electron transfer from the TiO₂ conduction band to the oxidized sensitizer. An IPCE of ∼24% at 690 nm and an overall conversion efficiency of 0.54% were achieved for a cell based on a ZnPcTyr-sensitized TiO₂ electrode, which is one of the best results reported for a photovoltaic device based on phthalocyanine. Adding TBP to the electrolyte decreases the IPCE, J_{SC}, and η considerably, although it increases somewhat the U_{OC}. In comparison with the data for a RuN3-sensitized TiO₂ thin film, electron injection is somewhat faster (completes

(34) It was found that the ZnPcTyr⁺ has absorption in the near-IR spectral region, similarly to Ru phthalocyanines.[35]
(35) Charlesworth, P.; Truscott, T. G.; Brooks, R. C.; Wilson, B. C. *J. Photochem. Photobiol. B: Biol.* **1994**, *26*, 277.
(36) Kallioinen, J.; Benkö, G.; Sundström, V.; Korppi-Tommola, J. E.; Yartsev, A. P. Submitted for publication.

in ~500 fs), charge recombination is much faster, and more than half of the injected electrons recombine with the oxidized dye in ~300 ps. Surface aggregation and fast charge recombination are responsible for the low IPCE, ϕ, and η of the solar cell based on ZnPcTyr.

To further improve the performance of phthalocyanine-based TiO_2 solar cells, some other redox-active substituents than tyrosine should be incorporated into the phthalocyanine macrocycle. Besides making the dye soluble in organic solvents and avoiding surface aggregation, the substituent should have an oxidation potential more negative than that of phthalocyanine to suppress the back-electron transfer from the conduction band of the semiconductor to the oxidized dye.

JA0178012